



Integrated Project - EUWB

Contract No 215669

Deliverable

D2.3.2

Radio environment map

Contractual data:	M40
Actual data:	M40
Authors:	GIORGETTI Andrea (UNIBO), PIERROT Jean-Benoît (CEA), WAADT Andreas (UDE), WANG Shangbo (UDE)
Participants:	CEA, UNIBO, UDE
Work package:	WP2
Security:	PU
Nature:	Report
Version:	1.0
Total number of pages:	42

Abstract

In this deliverable, we defined the problem of the estimation of the Radio Environment Mapping (REM) over a two-dimensional space with the use of a cognitive radio network with nodes capable to perform spectrum sensing. In order to address the problem the mean-square error (MSE) in the reconstructed REM and the optimal CR nodes density is considered in which we evaluated the best trade-off in terms of observation, sampling and quantization noises. A second method is proposed which also uses the spectrum sensing network of nodes. It evaluates an interference map of one or several OFDM-based emitters. This map is obtained at each node level in a distributed manner and can be used to find the places where emitters have a reduced effect on communication systems. Finally, a last method is described which proposes an optimal power allocation (OPA) scheme using the environment activity sensing and interferences awareness.

Keywords

Localization, regularization, tracking, interferers, cognitive, radio, power allocation, optimization

Table of Contents

1	Executive summary	6
2	Introduction	7
3	Radio Environment Map estimation through a Cognitive Radio Network	8
3.1	Decentralized Estimation.....	9
3.1.1	Spatial Field Model	9
3.1.2	Spatial Field Observation	10
3.1.3	Building the Radio Environment Map.....	11
3.2	Derivation of the REM Estimation Error.....	14
3.3	Particular case: Orthogonal Band-limited AWGN Channels	15
3.4	Numerical examples for a typical EUWB scenario	15
3.5	Conclusions	17
4	Kernel based radio environment reconstruction	18
4.1	Channel propagation model.....	18
4.2	Regularization.....	20
4.3	Distributed strategy and model order reduction	21
4.4	Numerical example.....	23
4.5	Conclusion.....	25
5	Power allocation scheme exploiting interference awareness.....	26
5.1	Overview	26
5.2	System model and network structure.....	27
5.3	Multi user receivers	27
5.3.1	Fundamentals.....	27
5.3.2	Multiuser rake receiver	28
5.3.3	Successive maximum likelihood receiver	30
5.4	Optimal power allocator	33
5.4.1	Fundamentals.....	33
5.4.2	Determine the Minimum Transmission Power of each User.....	34
5.4.3	Find the optimum transmission power of each user iteratively	35
5.4.4	Computational complexity of optimal power allocation	35
5.5	Simulation results	35
6	Conclusion.....	37

7 Appendix 38

 7.1 Annex 1 38

8 References 40

9 Acknowledgement 42

List of Figures

Figure 1: Illustration of the system model considered.....	10
Figure 2 : Schematic of the components which are present in the spectrum of the sampled signal.....	13
Figure 3: Normalized MSE as a function of the density ρ for different values of W and ε	16
Figure 4: Normalized MSE as a function of the density ρ for different values of OSNR γ	17
Figure 5: Interference sensing scenario	18
Figure 6: h channel response and the spatially correlated shadowing effect s	19
Figure 7: Regularized shadowing map	21
Figure 8: Algorithm applied on the way started by node 1.	23
Figure 9: Evolution of the error as a function of the bandwidth of the Laplacian kernel.....	24
Figure 10: Three emitters and the regularized map	25
Figure 11: Centralized UWB network structure.....	27
Figure 12: Structure of transmitted frame	31
Figure 13: Bit error ratio of the 22-finger rake receiver and the SML receiver	36
Figure 14: Overall throughput of OPA and MPA for different number of active users	36

Abbreviations

AWGN	Additive White Gaussian Noise
CKF	Cubature Kalman Filter
CR	Cognitive Radio
EC	European Commission
EUWB	CoExisting Short Range Radio by Advanced Ultra-WideBand Radio Technology
EKF	Extended Kalman Filter
GM	Gaussian Mixture
ie	Information Element
iid	Independent and Identically Distributed
KF	Kalman Filter
MAC	Medium Access Control Layer
MIMO	Multiple Input Multiple Output
ML	Maximum Likelihood
MTT	Multi Targets Tracking
OFDM	Orthogonal Frequency Division Multiplexing
PDP	Power Delay Profile
PHD	Probability Hypothesis Density
PHY	Physical Layer
PU	Primary User
RFS	Random Finite Sets
RSS	Received Signal Strength
RSSI	Received Signal Strength Indicator
RSSID	Received Signal Strength Indicator Difference
STT	Single Target Tracking
Wi-Fi	Wireless Fidelity
WSN	Wireless Sensor Network

1 Executive summary

Radio environment map (REM) building requires deployment of sensors according to cost, opportunity and performance constraints. In this deliverable, we propose three methods for REM. In first method, we address the specific case of a wireless sensor network (WSN), where CR nodes are randomly deployed with given uniform density, which performs random sampling of a l -dimensional signal over a limited domain area. A dense sensor deployment could ensure a large number of samples received by the collector, and hence an accurate estimate of the PU signal strength is estimated. However, due to a constraint on the overall bandwidth, a sparse deployment results in higher data rates for each dedicated channel, allowing for a fine-grained quantization of the measures. In this method, the problem of estimating a spatial field through a wireless sensor network with randomly distributed nodes has been considered. By assuming limited bandwidth and uniform quantization, we have derived analytical expressions for the MSE of the reconstructed signal as function of sensor density. The equation emphasizes the contributions of both quantization error (increasing vs ρ) and aliasing error (decreasing vs ρ), and permits the optimization of deployment density. A simplified closed-form expression for the MSE in the particular case of orthogonal AWGN bandwidth limited channels has also been provided.

We also propose another method to obtain radio environment map that relies on a wireless sensor network where each node has a sensing capability in the monitored frequency band. An assumption is made on the separation of bands between the measured interferers and WSN communication system. The main idea of this method is to obtain several maps, one per standard provided by the signal sniffer algorithm. Afterward, we show how to build a map of received signal from one emitter. The principle can also be generalized with several nodes using the same OFDM standard.

In the second method, we show that regression can take advantage of properties of the sparse representations with kernel machine. Based on performances require by the application, this method gives an interesting solution to reduce the number of parameters which describe a map but also decrease the quantity of information exchanged between nodes. This solution offers a good genericity (others kernels can be used if spatial correlation is not a constraint) and can model a large spectrum of environment activities. Therefore, the measure must have properties which stay inside the spatial and temporal sampling mathematical limits (ie Shannon). The spatial limits are given by the density of nodes in the network. The time boundaries are mainly due to the algorithm convergence speed. The future works have to concentrate on a method which can monitor the evolution of the measures due to the mobility of the nodes and radio environment dynamic using spatial and temporal kernels.

Finally, the last method proposes an optimal power allocation (OPA) scheme using the environment activity sensing and interferences awareness.

2 Introduction

At first in this document, we address the problem of the estimation of the REM defined over a two-dimensional space with the use of a cognitive radio network with nodes capable to perform spectrum sensing. We assume that the field is sampled by a set of cognitive nodes which are randomly deployed in a given geographical area, and sent to a fusion center (FC) to reconstruct the REM.

To address a realistic scenario, we impose a total bandwidth constraint which forces the quantization error in the CR node-to-FC channels to depend on the actual number of nodes in the network. With these assumptions, we derive the mean-square error (MSE) in the reconstructed REM and, on that basis, the optimal CR nodes density which attains the best trade-off in terms of observation, sampling and quantization noises. Results illustrate the dependency of the optimal operating point on the variance of the observation noise or the signal-to-noise ratio in the CR node-to-FC channels.

A second method is proposed which also use the spectrum sensing network of nodes. It evaluates an interference map of one or several OFDM-based emitters. This map is obtained at each node level in a distributed manner and can be used to find the places where emitters have a reduced effect on communication systems.

The method use a kernel based regularization solution. The communication channel is assumed to be spatially correlated to offer the same configuration met in indoor environments. We show due to the correlation we have to define a particular kernel. We describe the distributed method to build the map and finally we propose to use the mapping strategy when several emitters are active at the same time.

At last, to reduce harmful interference and improve coexistence, the knowledge of interferers' distribution is fundamental. A radio environment map, including interferers and a distribution of power densities, enables efficient CR strategies to maintain the network's quality of service (QoS) and to optimize the overall throughput. Those CR strategies include spatial recourse management like optimal power allocation schemes, which exploit and benefit from the radio mapping of CR devices and interferers. Chapter 5 discusses such an optimal power allocation (OPA) scheme with interference awareness. The OPA has been analyzed theoretically and by software simulations. It is shown that the interference aware OPA outperforms a conventional maximum power allocation (MPA) scheme, which has no knowledge about the radio environment. The used optimization constraints are 1) the maximal transmission power must not exceed the EMC limits; 2) the minimal transmission power must provide a certain minimal level of QoS at each receiver; 3) the overall throughput of the network shall be maximized. The simulation model, applied in this research, includes UWB multi-path propagation channels, IEEE 802.15.4a compliant UWB networks with multi-user scenarios and synchronization mismatch of UWB nodes, as well as different receiver structures, a rake receiver and a successive maximum likelihood (SML) receiver. It can be seen that the advantage of the OPA increases with increasing number of active users, i.e. with increasing number of interferers.

3 Radio Environment Map estimation through a Cognitive Radio Network

Radio environment map (REM) building requires deployment of sensors according to cost, opportunity and performance constraints. The problem considered is the estimation of a scalar field, such as the received power from a primary user (PU), in a wide area through the deployment of a cognitive radio network (CRN) where nodes are capable to perform received signal power measurement through spectrum sensing. CR nodes sense the received power level and transmit measurement results over band-limited channels to the collector (sometimes also called monitor or supervisor or base station (BS)), which usually consists of a device with increased functionalities and complexity. The latter is then in charge of reconstructing the original signal strength based on the received samples.

A variety of applications have been envisaged using wireless sensor networks (WSN), ranging from oceanography to building science and forest fire prevention [1][2][3]. Some of them simply aim at comparing the scalar field with given thresholds [2], whereas many others require the estimation of the entire behavior of the scalar field (in EUWB scenario the REM) [4][5]; the latter is the case investigated here. In the recent literature, different works addressed the estimation of a scalar or vectorial parameter using WSN. In [6], the authors address parameter estimation and derive an optimal quantization step, given a bandwidth constraint. Xiao *et al.*[7] present an optimal power scheduling strategy for decentralized estimation of a noise-corrupted source via wireless sensor network. In [8], estimation of a parameter is performed when multiple noisy observations are available. The authors also analyze a coding strategy that uses correlation information for a greater energy/bandwidth efficiency. The aforementioned works aim at estimating a scalar parameter observed by all the nodes.

Only few examples in the literature consider the estimation of a spatial field. Zhang *et al.* [9] consider a Kalman-Bucy filter based approach for the problem of estimating a time-varying real-valued random field with noisy measurements taken at equally spaced locations. In addition they assume the dynamics of the process to be estimated are described by a linear differential equation. In [4], source coding of correlated sources is considered in order to reduce the quantization error when transmitting over non-ideal channels. The latter work only focuses on quantization issues and considers a simple bivariate gaussian random variable (RV) with known covariance as source signal. In [5], the authors consider the exploitation of spatio-temporal dependencies to improve the power efficiency of the sensors. However, they base their analysis on an underlying Markov Random Field.

In this deliverable we address the specific case of a WSN, where CR nodes are randomly deployed with given uniform density, which performs random sampling of a l -dimensional signal over a limited domain area. A dense sensor deployment could ensure a large number of samples received by the collector, and hence an accurate estimate of the PU signal strength. However, due to a constraint on the overall bandwidth, a sparse deployment results in higher data rates for each dedicated channel, allowing for a fine-grained quantization of the measures. We emphasize that correlation information is not accounted for in our model. Although the latter leads to a more efficient estimation when the correlation law is known a priori (or when side information is exchanged between nodes, see e.g. [10]), the aim here is to keep the framework as general as possible by not conditioning on a particular source signal. Our main contribution is to compute the MSE in the reconstruction of the original PU signal level and to show the existence of an optimal deployment density that trades off between quantization error and aliasing error due to random sampling, thus extending the preliminary work [3]. We do so by using the theory of random sampling and allowing for linear quantization.

3.1 Decentralized Estimation

3.1.1 Spatial Field Model

The PU received power to be sampled is described here through the (target) l -dimensional spatial field $z(s)$ (s being the spatial variable). For example, signal $z(s)$ could represent a realization of a spatial random process $Z(s)$. Without loss of generality, we consider \mathbf{A} to be a ball of radius R and Lebesgue measure $\mu(\mathbf{A}) = A$, containing the part of the target signal monitored by the WSN. Hence, the actual (truncated) signal of interest is $x(s) = z(s) \cdot r_A(s)$, with

$$r_A(s) = \begin{cases} 1 & s \in \mathbf{A} \\ 0 & \text{otherwise} \end{cases} \quad (1)$$

and finite energy E_x .

We introduce the Fourier transform, $S_x(\nu)$, the autocorrelation function, $R_x(\tau)$, and the energy spectral density, $\mathbf{E}_x(\nu)$, of $x(s)$, as

$$S_x(\nu) = \mathfrak{F}^{(l)}[x(s)]; \quad (2)$$

$$R_x(\tau) = \int_{\mathbb{R}^l} x(s)x(s-\tau)ds; \quad (3)$$

$$\mathbf{E}_x(\nu) = \mathfrak{F}^{(l)}[R_x(\tau)], \quad (4)$$

respectively, where $\tau = (\tau_1, \tau_2, \dots, \tau_l)$ and $\nu = (\nu_1, \nu_2, \dots, \nu_l)$ is a spatial frequency. The operator $\mathfrak{F}^{(l)}[\cdot]$ represents the l -dimensional Fourier transform. In the following we will indicate the statistical expectation with $\mathbf{E}\{\cdot\}$.

We assume that $z(s)$ is band-limited, i.e., $S_z(\nu) = \mathfrak{F}^{(l)}[z(s)]$ does not contain significant spectral components outside \mathbf{S}_0 , where $\mathbf{S}_0 = \{\nu \text{ s.t. } (-B_z < \nu_1 < B_z, -B_z < \nu_2 < B_z, \dots, -B_z < \nu_l < B_z)\}$ and B_z represents the bandwidth per dimension of $z(s)$. The Fourier transform of $x(s)$ is then

$$S_x(\nu) = S_z(\nu) \otimes R_A(\nu), \quad (5)$$

where $R_A(\nu) = \mathfrak{F}^{(l)}[r_A(s)]$ and \otimes is the convolution operator. In the practical bi-dimensional case ($l = 2$) we have

$$R_A(\nu) = \frac{R}{\|\nu\|} J_1(2\pi R \|\nu\|), \quad (6)$$

where $J_1(\cdot)$ is the Bessel Function of the first kind of order one and $\|\cdot\|$ is the norm operator. Note that, due to the spatial truncation of the original signal, $x(s)$ is not bandlimited. However, it can be easily verified that $R_A(\nu) \approx 0$ when $\|\nu\| > 1/\pi R$. In general, $S_x(\nu)$ and, therefore, $E_x(\nu) \approx 0$ outside \mathbf{S} , where $\mathbf{S} = \{\nu \text{ s.t. } (-B < \nu_1 < B, -B < \nu_2 < B, \dots, -B < \nu_l < B)\}$ and, in the two-dimensional case, $B = 1/\pi R + B_z$. The Lebesgue measure of \mathbf{S} is $\mu(\mathbf{S}) = \beta$, where $\beta = (2B)^l$ represents the minimum Nyquist sampling rate in the case of uniform sampling of $x(s)$ [11][12]. In practical applications we have $1/\pi R \leq B_z$, that is the area of observation is chosen larger than the typical spatial correlation distance which is proportional to $1/B_z$.

3.1.2 Spatial Field Observation

We consider a scenario where nodes are randomly deployed according to a homogeneous PPP with spatial density ρ (see Figure 1).

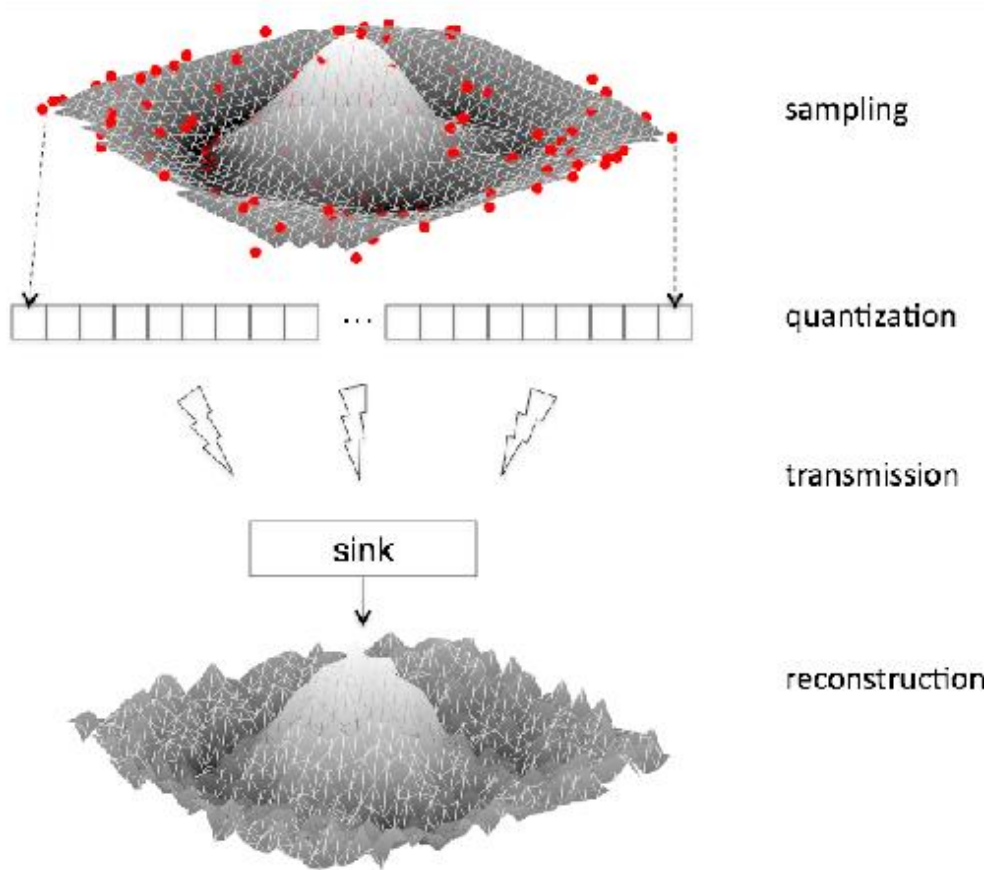


Figure 1: Illustration of the system model considered.

Therefore, by fixing the observation area A and the node density ρ , it turns out that the number K of active nodes transmitting a sample is a RV with expectation $\mathbf{E}\{K\} = \rho A$ and Poisson distribution given by [1]

$$p_K(k) = \Pr\{K = k\} = \frac{(\rho A)^k}{k!} e^{-\rho A}. \quad (7)$$

The k th node is located in the spatial point s_k and makes the observation $x_k = x(s_k)$ at sampling rate R_s samples/s. Assume that sensor measurements have a dynamic range such that $x_k \in [-M, M]$. The observations are then corrupted by additive noise, that is, $r_k = x_k + n_k$, for $k = 1, 2, \dots, K$, where $\{n_k\}$ are independent Gaussian RV with zero mean and variance η_k^2 . Define $\gamma_k = E_x / \eta_k^2$ as the average observation signal-to-noise ratio (OSNR) of the k th sensor.

Each node quantizes the observed sample and generates a discrete message $y_k = y_k(x_k, m_k)$ of m_k bits (uniform quantization) using $L_k = 2^{m_k}$ quantization levels. The value of the k th message can be represented as $y_k = x_k + n_k + v_k$, where the quantization noise $v_k = v_k(x_k, m_k)$ is such that $|v_k| \leq M / L_k$. Since the uniform quantizer is unbiased, we have $\mathbf{E}\{y_k\} = x_k$ and variance $\mathbf{V}\{y_k\} = \sigma_k^2$. It can be shown that $\sigma_k^2 \leq q_k^2 + \eta_k^2$, where [7]

$$q_k^2 = \frac{M^2}{(2^{m_k} - 1)^2}. \quad (8)$$

3.1.3 Building the Radio Environment Map

Starting from the collected samples, the goal is to obtain an estimate $\hat{X}(s)$ of the target signal $x(s)$. Conditioned on signal $x(s)$, samples y_k are independent and hence the best linear estimate \hat{x}_k of the k th sample is simply $\hat{x}_k = y_k$, which results to be unbiased. The normalized MSE in the estimate of sample x_k is given by

$$D_k = \frac{1}{E_x} \mathbf{E}\{(\hat{x}_k - x_k)^2\} = \frac{\sigma_k^2}{E_x} \leq \frac{1}{\gamma_k} + \frac{q_k^2}{E_x} \frac{1}{\gamma_k} + \frac{F_p}{(2^{m_k} - 1)^2} \quad (9)$$

with $F_p = M^2 / E_x$ being the peak factor of the sampled field.

For further convenience, we define the MSE averaged over the number of nodes K , i.e.,¹

$$\bar{D} = \sum_{K=1}^{\infty} p_K(K) \sum_{k=1}^K D_k. \quad (10)$$

Recalling that sensors are distributed according to a PPP, the derivative of the corresponding counting process is the stationary random process with mean $\mu_p = \mathbf{E}\{P(s)\} = \rho$ and statistical autocorrelation function and power spectral density given by [11][13]

$$R_p(\tau) = \rho \cdot \delta(\tau) + \rho^2, \quad (11)$$

$$S_p(\nu) = \rho + \rho^2 \cdot \delta(\nu), \quad (12)$$

respectively, where $\delta(\cdot)$ is the Dirac pseudo function. $P(s)$ represents the sampling process. The sampled version $H(s)$ of the target signal conditioned to the realization $x(s)$, can be expressed as $H(s) = x(s) \cdot P(s)$, representing a finite energy non stationary random process. We can represent the signal at the fusion center as

$$Y(s) = \sum_k y_k \delta(s - s_k) = H(s) + W(s), \quad (13)$$

where $W(s) = \sum_k w_k \delta(s - s_k)$, $w_k = n_k + v_k$, and $H(s) = \sum_k x_k \delta(s - s_k)$.

Let us now define the average statistical autocorrelation function of $Y(s)$ as

$$\bar{R}_Y(\tau) = \int_{\mathfrak{R}^d} \mathbf{E}\{Y(s)Y(s-\tau)\} ds = \bar{R}_H(\tau) + \bar{R}_W(\tau), \quad (14)$$

where $\bar{R}_H(\tau)$ and $\bar{R}_W(\tau)$ denote the average statistics autocorrelation function of $H(s)$ and $W(s)$, respectively. $\bar{R}_H(\tau)$ can be written as

$$\bar{R}_H(\tau) = \int_{\mathfrak{R}^d} \mathbf{E}\{x(s)x(s-\tau)P(s)P(s-\tau)\} ds$$

¹The two summations in (10) should start at $k, K = 0$. However, since to the best of Authors' knowledge there is no meaningful way to define the MSE when no sensors are present in the monitored area, we take $k, K > 0$. Equation (10) still has sense provided that $\mathbf{E}\{K\} = \rho A \gg 1$.

$$= \int_{\mathbb{R}^+} x(s)x(s-\tau)R_p(\tau)ds = R_p(\tau) \cdot R_x(\tau). \quad (15)$$

The average energy spectral density is then

$$\bar{E}_H(\nu) = \mathfrak{F}^{(l)}[\bar{R}_H(\tau)] = E_x(\nu) \otimes S_p(\nu). \quad (16)$$

From (11), (15) and (16) it follows

$$\bar{E}_H(\nu) = \rho^2 E_x(\nu) + E_x \cdot \rho \quad (17)$$

$$\bar{E}_Y(\nu) = \rho^2 E_x(\nu) + E_x \cdot \rho + \bar{E}_w(\nu) \quad (18)$$

where $\bar{E}_w(\nu) = \mathfrak{F}^{(l)}[\bar{R}_w(\tau)]$ and $\bar{E}_Y(\nu)$ is the average spectral density of $Y(s)$. Looking at (18), it is worthwhile noting that the spectrum of the sampled signal is composed of three components. The first one is proportional to the spectrum of the sampled signal $x(s)$ and represents the useful term. The second component represents the white aliasing noise, that arises, even for arbitrarily large nodes densities, due to the random nature of sampling. The last component accounts for both quantization and observation noise.

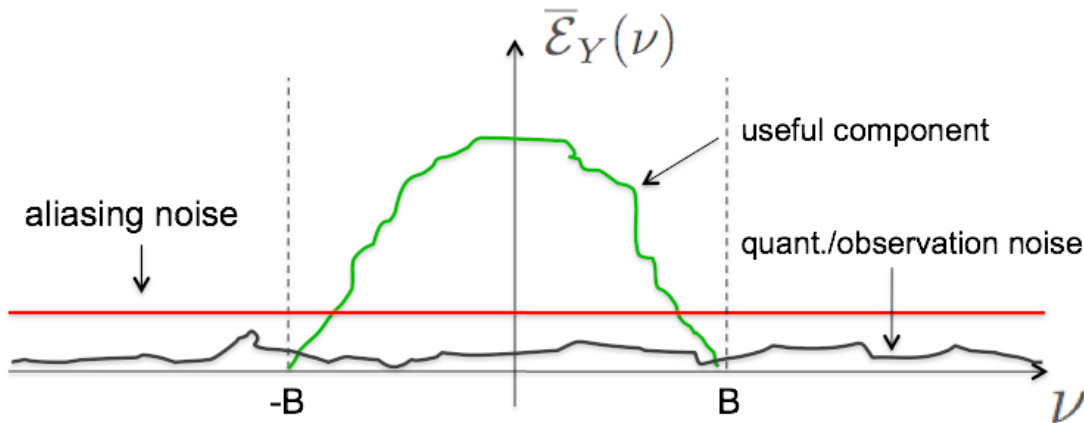


Figure 2 : Schematic of the components which are present in the spectrum of the sampled signal.

The 1-dimensional case is considered for the sake of illustration.

It is clear from (18) and from Figure 2 that the estimated signal can be reconstructed from its samples by means of an ideal low-pass filter that separates the useful bandwidth component from part of the noise. Therefore the estimate $\hat{X}(s)$ can then be expressed as

$$\hat{X}(s) = \phi(s) \otimes Y(s) = \sum_k x_k \phi(s - s_k) + \sum_k w_k \phi(s - s_k), \quad (19)$$

where $\phi(s)$ is the impulse response of the linear interpolator, whose transfer function $\Phi(\nu) = \mathfrak{F}^{(l)}[\phi(s)]$ is given by

$$\Phi(\nu) = \begin{cases} 1/\rho & \nu \in \mathbf{S} \\ 0 & \text{otherwise} \end{cases} \quad (20)$$

and represents the case of an ideal low-pass interpolator. The normalization factor $1/\rho$ in (20) has been considered to have a useful component at the output with energy E_x .

3.2 Derivation of the REM Estimation Error

As an indicator of the estimation quality, we consider the average normalized estimation error defined as the normalized MSE

$$\text{MSE} = \frac{1}{E_x} \mathbf{E} \left\{ \int_{\mathfrak{R}^l} (\hat{X}(s) - x(s))^2 ds \right\} \quad (21)$$

After some rearrangement shown in the Appendix, (21) results in

$$\text{MSE} = \frac{\beta}{\rho} \left(1 + \frac{1}{\rho} \bar{D} \right) \quad (22)$$

where \bar{D} is given by (10). Eq. (22) gives a general relationship between the estimate quality in terms of MSE, the node density, the process bandwidth, and the average distortion in single samples estimate.

3.3 Particular case: Orthogonal Band-limited AWGN Channels

Here we provide an example on how the result in (22) can be applied to a specific scenario characterized by the availability of orthogonal AWGN channels with total available bandwidth W . Additionally, we let the OSNR be $\gamma_k = \gamma$, $\forall k$, the received power $P_{rx,k} = P_{rx}$, $\forall k$ and the number of quantization bits $m_k = m$, $\forall k$, for simplicity. Under bandwidth constraint W , the transmission rate R_k of each node is limited by the channel capacity. Specifically, a fixed maximum number of orthogonal channels N_ε at constant bit rate $R_k = R$, is envisaged. As a consequence, if K exceeds N_ε the system results to be in outage. We define N_ε such that

$$\Pr\{K > N_\varepsilon\} < \varepsilon, \quad (23)$$

where $\varepsilon = 1$. Then the following upper bound on the rate

$$R = R_s m \leq \frac{W}{N_\varepsilon} \log_2(1 + \text{SNR} \cdot N_\varepsilon), \quad (24)$$

where $\text{SNR} = P_{rx}/(N_0 W)$, holds with confidence $(1 - \varepsilon)$. In practice, ε represents the probability that the network cannot satisfy the required capacity (outage probability). From (9) and (10) it turns out that

$$\bar{D} = \rho A \left(\frac{1}{\gamma} + \frac{F_p}{(2^m - 1)^2} \right) \quad (25)$$

with $m = W / R_s N_\varepsilon \log_2(1 + \text{SNR} \cdot N_\varepsilon)$. Finally, from (25), (22) and (24), the MSE, when the system is not in outage, is

$$\text{MSE} = \frac{\beta}{\rho} \left(1 + \frac{A}{\gamma} + \frac{A F_p}{(2^m - 1)^2} \right). \quad (26)$$

It is important to note that, for fixed ε and N_ε , parameter m depends on ρ and hence in (26) an optimization problem arises as will be shown in the numerical results.

3.4 Numerical examples for a typical EUWB scenario

In Figure 3 we show the MSE as a function of sensors density ρ , for the 2-dimensional case and different values of the total available bandwidth W and outage probability $\varepsilon = 0.1, 0.01$. The observable general trend suggests that the error initially drops when increasing ρ . This is because a more dense sampling helps reconstructing the original signal by decreasing the aliasing noise. However, bandwidth constraints impose a lower bit rate when a great number of sensors transmit simultaneously. As a consequence, larger ρ implies larger quantization noise, since each node is forced to quantize more loosely to cope with limited transmission rate. Hence, the plot highlights an optimum sensor density, ρ_{opt} , that trades off between

aliasing and quantization noise. It can also be seen that smaller outage probability (i.e., $\varepsilon = 0.01$) results in poorer performance. The reason of this is that smaller ε implies a greater number of allocated channels which, in turn, have smaller bandwidth. As a consequence, nodes are forced to increase the quantization step thus making quantization noise the dominant degradation cause. However, the system can manage a larger number of sensors and is less likely to incur in outage events.

We report in Figure 4 the MSE as a function of ρ , for different values of the OSNR γ . Clearly, when sensory observations are not significantly affected by noise, lower MSE values can be achieved. In particular, if γ increases from 10 to 1000, the MSE decreases by almost two decades. The optimal density, ρ_{opt} , does depend on γ , as expected. In fact, when samples are more corrupted by observation noise, the optimum moves to the right, meaning that a finer sampling is required (although additional noise occurs due to quantization). Finally, the curves get flatter for smaller γ . This implies the existence of a wider range of suboptimal density values that result in slightly poorer performance but allow for remarkable savings in terms of deployment cost.

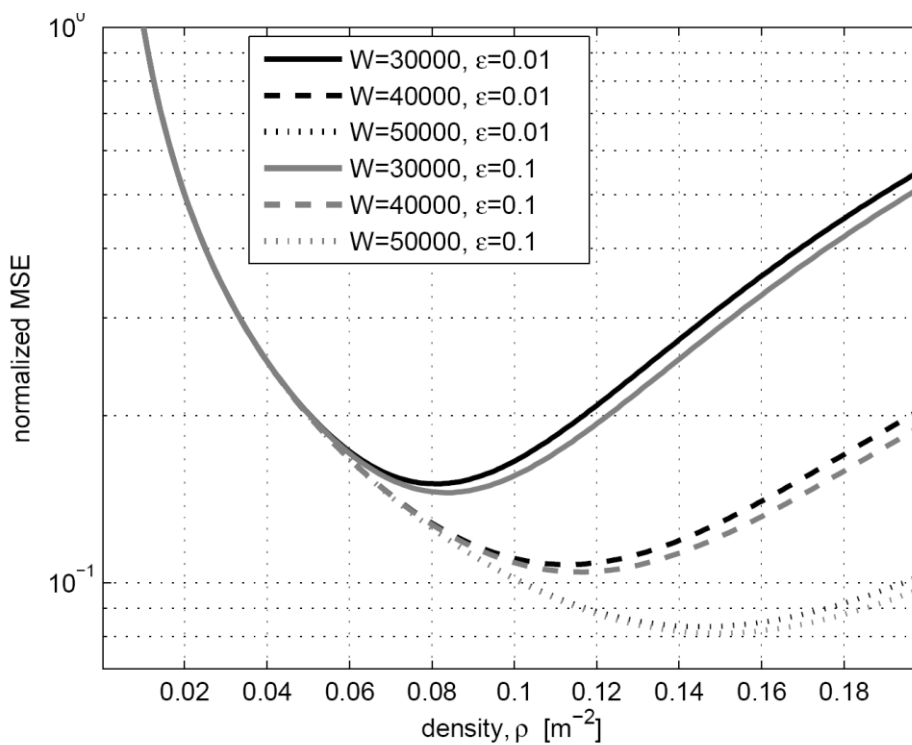


Figure 3: Normalized MSE as a function of the density ρ for different values of W and ε .

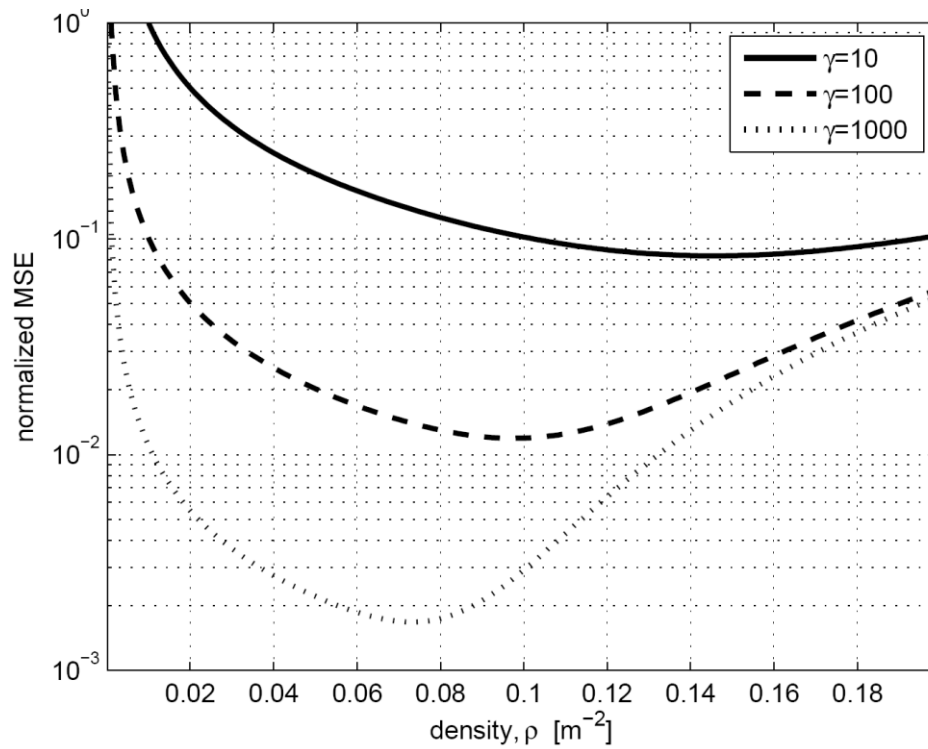


Figure 4: Normalized MSE as a function of the density ρ for different values of OSNR γ .

3.5 Conclusions

The problem of estimating a spatial field through a wireless sensor network with randomly distributed nodes has been considered. By assuming limited bandwidth and uniform quantization, we have derived analytical expressions for the MSE of the reconstructed signal as function of sensor density. The equation emphasizes the contributions of both quantization error (increasing vs ρ) and aliasing error (decreasing vs ρ), and permits the optimization of deployment density. A simplified closed-form expression for the MSE in the particular case of orthogonal AWGN bandwidth limited channels has also been provided.

4 Kernel based radio environment reconstruction

Obtaining a view of the interferences map of several standards is an interesting thing for the ones who are searching to help the base station deployment process or guide the mobile user to the best place for an optimal signal reception. In this chapter we propose a method to obtain this map that relies on a wireless sensor network where each node has a sensing capability in the monitored frequency band. An assumption is made on the separation of bands between the measured interferers and WSN communication system. Of course, for the following method we have the similar issues as described in the introduction of the previous chapter (§3).

Our scenario is based on a wireless sensor network (WSN) deployed in an indoor space. In the following studies we use the signal measurement extracted using the technique already described in a previous deliverable of the project and publication [16]. The main idea is to obtain several maps, one per standard provided by the signal sniffer algorithm (cf Figure 5). In the next section we show how to build a map of received signal from one emitter as shown in Figure 5. The principle can also be generalized with several nodes using the same OFDM standard. Some results are shown at the end of the chapter.

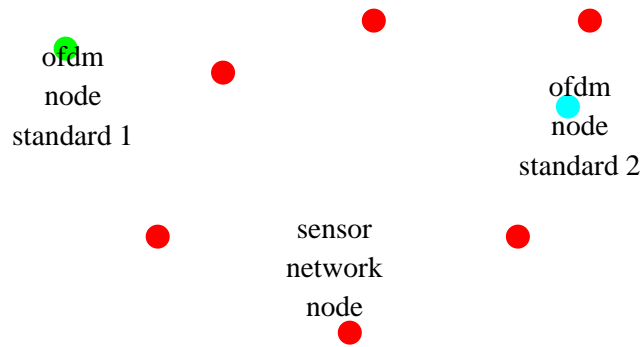


Figure 5: Interference sensing scenario

4.1 Channel propagation model

For our experiments we use a statistical model based on the radio channel proposed by Suzuki [22]. In Suzuki's model, the amplitude of the channel is a product of a Rayleigh process and a log-normal process. The Rayleigh distributed process accounts for fading and is the envelope of a complex Gaussian random process. Here it is not assumed and we keep only the first part of the model with the log-normal process:

$$h(p_t, p_r) = e^{\mu(p_t, p_r) + \xi_{PL}s(p_t, p_r)} \quad (27)$$

where shadowing process $s(\bullet)$ is a real Gaussian random process with zero mean and unit variance, the local mean $\mu(\bullet)$ reflects the effect of the path loss

$$\mu(p_t, p_r) = \underbrace{20 \log_{10} \left(\frac{4\pi d_0}{\lambda} \right)}_{P_0} - 10\alpha_{PL} \log_{10} \left(\frac{\|p_t - p_r\|}{d_0} \right) \quad (28)$$

and ξ is the standard deviation of the lognormal process whose typical values are:

- **Indoor LOS Channel:** The transmission channels between interferers in the same room of the sensors will essentially have a LOS Log-Normal channel. For typical LOS indoor Log-Normal

channels the values for the path loss exponent and the shadowing variance are in the range of $\alpha_{PL} = 1.6$ and $\xi_{PL} = 1.75$ (dB).

- **Indoor NLOS Channel:** The transmission channels between interferers in rooms, other than that where the sensors are, including obstacles such as walls etc. will essentially have a NLOS Log-Normal channel. For typical NLOS indoor Log-Normal channels the values for the path loss exponent and the shadowing variance are in the range of $\alpha = 3.6$ and $\xi = 3.75$ (dB).

Notice that normally Suzuki's channel model is a random function of time. But a 1D process cannot correctly capture the spatial correlation when a mobile user is moving along a curve rather than a straight line. This motivates the following 2-D lognormal process that depends on the user's location $p = (x; y)^T$.

In the regularization map building the shadowing process is offering a perturbation which is spatially correlated. This correlation is not really well specified in literature but an exponential form which fits well the measurement data is given by [23]:

$$\hat{s}(p_t, p_r) \rightarrow N(0,1) \quad (29)$$

$$E[\hat{s}(p_t, p_r)\hat{s}(p_t, p_r + \tau)] \approx e^{-\beta(\tau^T \tau)^{1/2}}$$

Our next step applies a regularization process which gives as output a estimated map f^* of the combination of interferences signal power. Now we assume for one kind of standard we have one emitter and a receiver located in p obtain something proportional to

$$f(p) \propto \mu(p_t, p) + \xi s(p_t, p) \quad (30)$$

And correlation on the log-channel is something proportional to

$$R(\tau) = E[h(p_t, p_r)h(p_t, p_r + \tau)] \propto |\mu(p_t, p_r)|^2 \delta(\tau) + \xi^2 e^{-\beta(\tau^T \tau)^{1/2}} \quad (31)$$

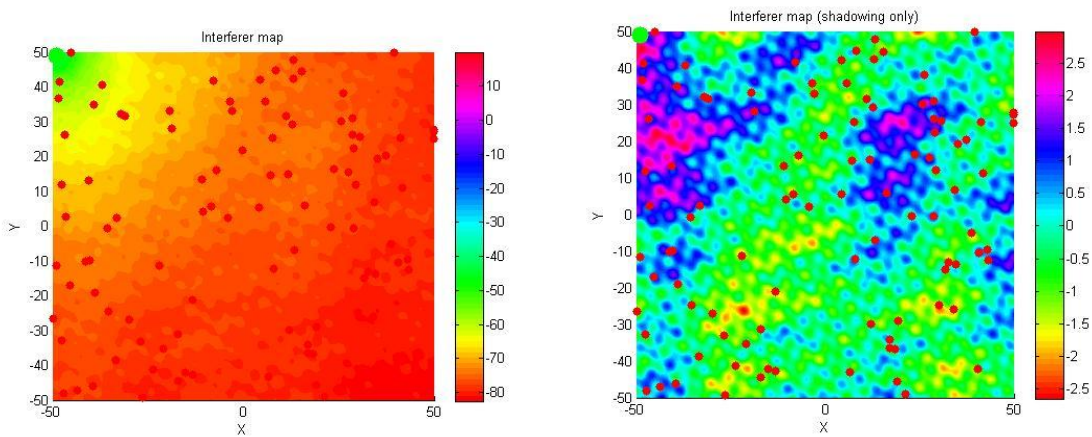


Figure 6: h channel response and the spatially correlated shadowing effect s

The h channel response (ie received signal – emitted signal 0dB, 100 nodes) (a) and the spatially correlated shadowing effect s (b). Emitter (green) and randomly deployed WSN nodes (red). (Figures are meshed using a grid 1000x1000, z values in dB)

4.2 Regularization

For the problem of modelling our physical phenomena we can use many approaches to address this issue with collaborative nodes in WSN. They have been proposed in the signal processing literature (see survey [24]). As the survey explained the different approaches highly depend on the modelling assumption but due to the complexity of channel changes in an indoor environment we investigate a model-independent method using reproducing kernel [25]. This method uses a distributed learning strategy where each node acquires information from neighbourhood to solve locally a least-squares problem. Nevertheless, the method is not suitable when the order of models scales linearly with the number of deployed sensors and measurements. We will propose (§4.3) a reduce model order by using appropriate sparsification criterion.

The RKHS solution to the regularization problem is a conventional regression which seeks a function that links the best the input space to the observation domain. We learn this function f^* from available data (p_i, d_i) for N different samples (or node location). The optimization problem is given by minimizing the mean square error between the model output $f(p_i)$ and the measured input d_i :

$$f^*(p) = \arg \min_{f \in H} \frac{1}{N} \sum_{i=1}^N |d_i - f(p_i)|^2 + \eta \|f\|_H^2 \quad (32)$$

This optimization is constrained into a functional space of smooth functions. It is a well-known problem in RKHS theory where quadratic form describes the fitting with the data and η controls the smoothness trade-off. In this expression, H (Hilbert space) is the RKHS of a given reproducing kernel κ . This means that each function of H is evaluated at any position with $f(p) = \langle f, \kappa \rangle_H$ (the inner product in H). The representer theorem [26] states that the solution of the previous regularized optimization problem is of the form:

$$f^*(p) = \sum_{i=1}^N \alpha_i \kappa(p_i, p) \quad (33)$$

The model completely identified by its coefficients α_i gives the dual optimization problem [27]

$$\mathbf{\alpha}^* = \arg \min_{\mathbf{\alpha} \in H} \frac{1}{N} \sum_{i=1}^N |\mathbf{d} - \mathbf{K}\mathbf{\alpha}|^2 + \eta \mathbf{\alpha}^T \mathbf{K}\mathbf{\alpha} \quad (34)$$

Where K is the N-by-N Gram matrix whose entries are $\kappa(p_i, p_j)$. \mathbf{d} and $\mathbf{\alpha}$ are column vector with size N and entries are d_i and α_i . It is a linear optimization problem and the solution is given by

$$\mathbf{\alpha}^* = (\mathbf{K}^T \mathbf{K} + \eta \mathbf{K})^{-1} \mathbf{K}^T \mathbf{d} \quad (35)$$

The next step is the design of a kernel function κ which defines the RKHS H and has an impact on the performances of the regularizer. The main idea [31] is to find a kernel which reproduces the properties of the original function. For a generic curve any kind of RKHS kernels can be used. The most classic examples are the radially Gaussian $\kappa(p, p') = e(-\|p - p'\|^2 / 2\sigma^2)$ or Laplacian $\kappa(p, p') = e(-|p - p'|/\sigma)$ (with $\sigma > 0$ the kernel bandwidth) kernels. In our case we proposed a constraint on the channel spatial correlation (29) and our kernel must have the appropriate properties to catch it. As shown in [28] the correlation function

can be used as the kernel for our optimization. Due to the form of the correlation (29) the best candidate under our hypothesis is the Laplacian kernel with $\sigma = 1/\beta$.

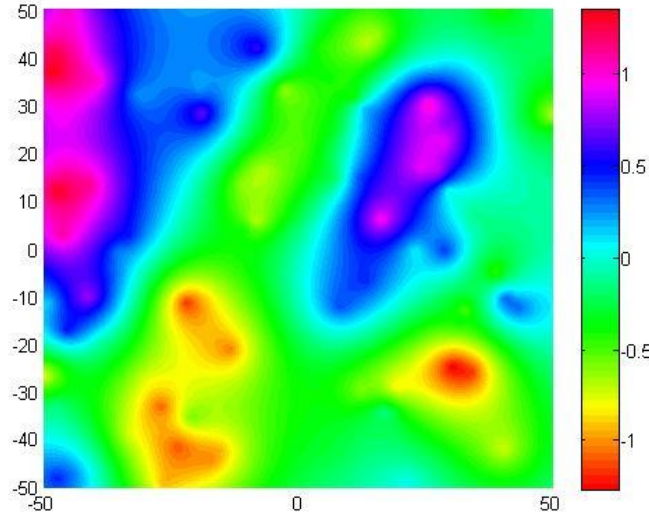


Figure 7: Regularized shadowing map

(based on example from Figure 6b), Laplacian kernel and $\beta = 0.1$.

4.3 Distributed strategy and model order reduction

The regularization technique based on optimization solution (35) assumes a centralized computation of the parameters. Our objective is to provide a map of their neighbourhood at each node level. In this study the surface covered by the map is not limited but for large network we have to specify distance limits to avoid a too large number of parameters. The choice of the limit depends mainly of the application requirements and users decision. Now, it is not in our scope.

The proposed method use a distributed strategy and a reduce-order model constructed from the optimal one (33) by considering only a small number of kernel functions. Now we consider that our model is reduced to an order M .

$$f(p) = \sum_{l=1}^M \alpha_l \kappa(p_{w_l}, p); M \leq N \quad (36)$$

Where coordinates p_{w_l} are selected from the locations of the nodes and w_l is the node reference at step l of the algorithm. We note that injecting (36) into (33) of the regularization problem we obtain a similar solution to (35) where we need to make the inverse of an M -by- M matrix with the entries $\kappa(p_{w_i}, p_{w_j})$. The next step is the method to select the appropriate series of M nodes given the successive position $\{p_{w_l}\}_{l=1..M}$. But before we have to determine an appropriate sparse representation which is not computational expensive [32] and with a criterion [31] that does not require the inversion of matrix. For this, we take advantage on the coherence criterion which keeps the kernel function $\kappa(p_l, p)$ into the M -order model if the cross-correlation measure is under a certain threshold θ .

$$\max_{l=1 \dots M} \left| \kappa(p_i, p_{w_l}) \right| \leq \theta \quad (37)$$

This criterion is related to the approximate linear dependence one [33] which is based on a simple walk through the network where each node discards its kernel function from the model, and thus leaves its order unchanged, if the kernel function can be well approximated by the model. Otherwise the order is incremented by adding the kernel function to the model. The approximate linear dependence criterion is

$$\min_{\beta} \left| \kappa(p_i, p) - \sum_{l=1}^M \beta_l \kappa(p_{w_l}, p) \right|^2 > \varepsilon \quad (38)$$

Basically this criterion requires a matrix inversion which is not required for the previous one.

In the particular case of the used Laplace kernel which can be expressed in terms of $\kappa(|p_i - p_j|)$, the criterion may be simplified by

$$\min_{l=1 \dots M} |p_i - p_{w_l}| \leq \eta = \sigma \log\left(\frac{1}{\theta}\right) \quad (39)$$

And finally we derive from the previous an algorithm to learn the reduced order model in a distributed manner. For this purpose, each node i updates the coefficient vector α_i to be as close as possible to the one at a previous step α_{i-1} . We have to solve the following constraint optimization problem

$$\begin{aligned} \min_{\alpha_i} & \|\alpha_i - \alpha_{i-1}\|^2 \\ \mathbf{\kappa}_i^T \alpha_i &= d_i \end{aligned} \quad (40)$$

With $\mathbf{\kappa}_i$ and M column vector whose entries are $\{\kappa(p_{w_l}, p_i)\}_{l=1 \dots M}$ and the constraint is obtained by applying (36) to information of node i . Solving this problem at each node depends if the criterion (39) is satisfied or not.

In the case when considered node i is in the neighbourhood of any of the m previously selected sensor we have $\min_{l=1 \dots M} |p_i - p_{w_l}| \leq \eta$. Its kernel function may be well approximated by a linear combination of the model kernel functions. The optimization problem solution is solved by considering minimizing the Lagrangian

$$\|\alpha_{i-1} - \alpha\|^2 + \lambda(d_i - \mathbf{\kappa}_i^T \alpha) \quad (41)$$

The zero value of the derivatives of the above cost function with respect to α and the Lagrangian multiplier λ get the following conditions on α_i

$$\begin{aligned} 2(\alpha_i - \alpha_{i-1})^T &= \lambda \mathbf{\kappa}_i^T \\ \mathbf{\kappa}_i^T \alpha_i &= d_i \end{aligned} \quad (42)$$

Because the matrix product of kernel vector κ_i is not null, the equations lead to $\lambda = 2(\kappa_i^T \kappa_i)^{-1} (d_i - \kappa_i^T \mathbf{a}_{i-1})^T$. The value $d_i - \kappa_i^T \mathbf{a}_{i-1}$ is the a priori error at node i. Finally we obtain the update equation in the first case

$$\mathbf{a}_i = \mathbf{a}_{i-1} + \rho \frac{\kappa_i}{\|\kappa_i\|^2} (d_i - \kappa_i^T \mathbf{a}_{i-1}) \quad (43)$$

ρ is the control parameter recommended in conventional adaptive filtering techniques.

The second case is the one when node I is not covered by the m sensors defining in the kernel function of the model. We have to increment the model order by including the corresponding kernel function to it. We modify the previous local minimization problem as

$$\begin{aligned} \min_{\mathbf{a}} & |\mathbf{a}_{i..M} - \mathbf{a}_{i-1}|^2 + \alpha_{M+1}^2 \\ & \kappa_i^T \mathbf{a}_i = d_i \end{aligned} \quad (44)$$

Where $\mathbf{a}_{i..M}$ denotes the M first elements of the vector and κ_i has been increased by one entry. Finally the updating step is given by

$$\mathbf{a}_i = \begin{bmatrix} \mathbf{a}_{i-1} \\ 0 \end{bmatrix} + \rho \frac{\kappa_i}{\|\kappa_i\|^2} \left(d_i - \kappa_i^T \begin{bmatrix} \mathbf{a}_{i-1} \\ 0 \end{bmatrix} \right) \quad (45)$$

κ_i is a M+1 column vector whose entries are $\{\kappa(p_{w_i}, p_i)\}_{i=1..M+1}$ and $w_{M+1} = i$.

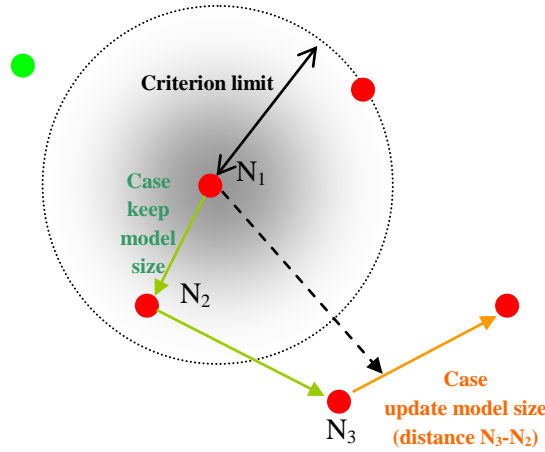


Figure 8: Algorithm applied on the way started by node 1.

4.4 Numerical example

For the numerical results we apply the method on the signal received from one emitter ($\alpha_{PL} = 2.0$, $\xi_{PL} = 1.0$). We have 100 nodes randomly deployed inside a square region with the border size equal to 100m. The emitter is located in the top left corner of the space. As described in §4.1 the channel is correlated

with a coherence parameter equal to 10m. The communication region between nodes is assumed Boolean with a radius of the circle adjusted to obtain an average of neighbours in communication inside the network equal to 5. The step size ρ is equal to 0.5 (several tests with values change [0.3 1.0] does not modify the next results).

To determine the influence of bandwidth σ parameter in the model we define the root mean square error by the difference of real value at several locations and the regularized value using the estimated model.

$$\int (f(p) - f^*(p))^2 dp \quad (46)$$

The result is given by Figure 9 for different σ values. As shown the optimal bandwidth is given by 10 which are related to the intrinsic correlation of the spatial function.

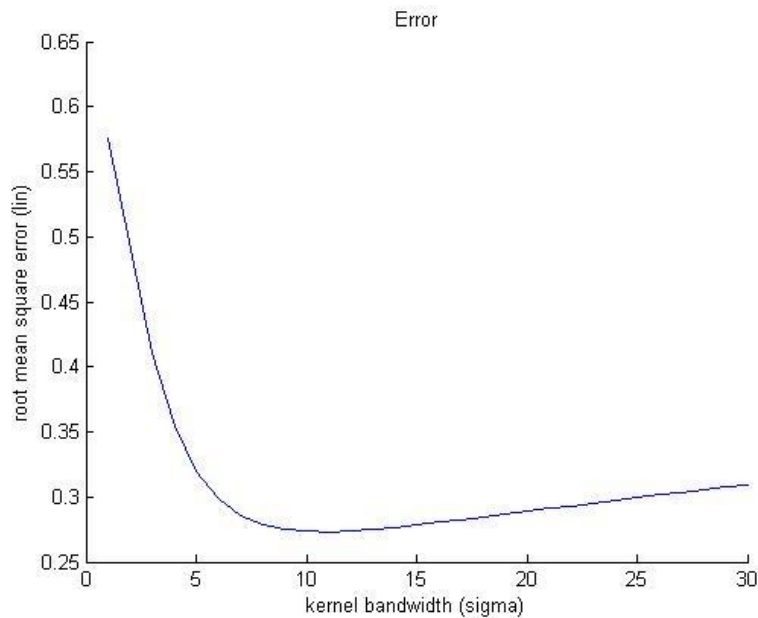


Figure 9: Evolution of the error as a function of the bandwidth of the Laplacian kernel.

The signal correlation parameter is 0.1 for the simulation.

For the case of several sources the analytical form is more complex because two similar OFDM signal have correlations together and the measurement [16] is biased by them. Therefore this information mapped by our method is useful for a user who is searching to minimize the influence of interferences in the same band and with the same norm. An example of such kind of map obtained with 3 interferences is shown in Figure 10.

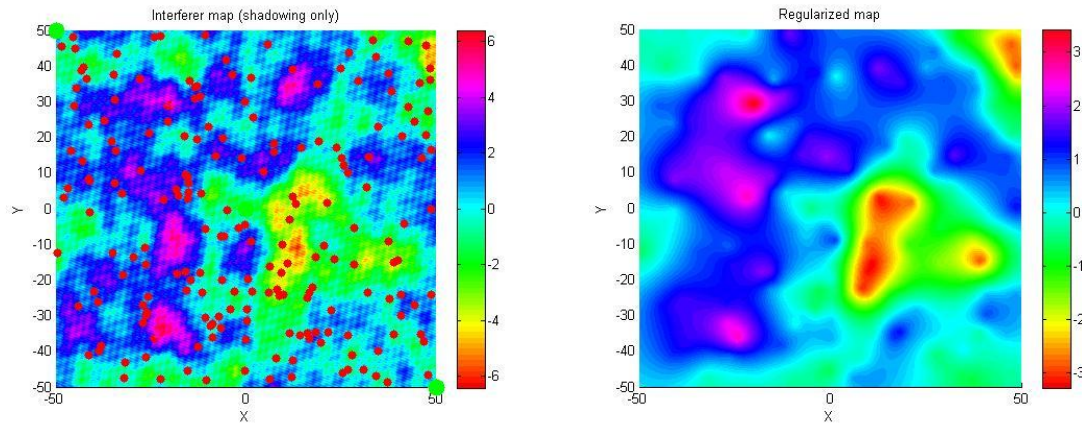


Figure 10: Three emitters and the regularized map

Three emitters (top-left, center, down-right) and resulting interferences (a).

The (b) is the regularized map obtained by the 100 nodes of the network.

4.5 Conclusion

In this section we showed that regression can take advantage of properties of the sparse representations with kernel machine. Based on performances require by the application, this method gives an interesting solution to reduce the number of parameters which describe a map but also decrease the quantity of information exchanged between nodes. This solution offers a good genericity (others kernels can be used if spatial correlation is not a constraint) and can model a large spectrum of environment activities. Therefore the measure must have properties which stay inside the spatial and temporal sampling mathematical limits (ie Shannon). The spatial limits are given by the density of nodes in the network. The time boundaries are mainly due to the algorithm convergence speed. The future works have to concentrate on a method which can monitor the evolution of the measures due to the mobility of the nodes and radio environment dynamic using spatial and temporal kernels.

5 Power allocation scheme exploiting interference awareness

5.1 Overview

The availability of a radio environment map and the knowledge about the received signal and interference powers at different communication nodes enables new strategies for spatial management and reuse of spectrum resources. If the radio resources are managed by a central network coordinator (NC), a centralized optimal power allocation (OPA) scheme could be used as an appropriate strategy to maximize the overall network throughput while insuring a certain quality of service (QoS) level for every single user.

In this research, OPA schemes with interference awareness are investigated and compared to a common maximum power allocation (MPA) mechanism. In the theoretical analysis and in software simulations, a centralized Impulses Radio Ultra-Wideband (IR-UWB) multi user system is considered, which contains one network coordinator (NC). Different receiver types are applied to a multipath scenario, a rake receiver and a successive maximum likelihood (SML) receiver. Compared to the MPA, the OPA with interference awareness increases the overall network throughput. In the OPA scenario, the SML receiver outperforms the rake receiver, if SNR knowledge is exploited.

To meet the QoS demands of each UWB user and maximize the overall network throughput, several technical aspects are considered, the physical layer transmission format, the multi user access format and routing schemes.

There are different modulation schemes used in UWB. For low data rate (LDR) UWB, pulse based modulation is commonly used. High data rate (HDR) UWB on the other hand uses orthogonal frequency division modulation (OFDM) [19]. This research focuses on LDR UWB network in which each UWB node uses a time hopping pulse position modulation (TH-PPM) as the physical layer transmission format. Time hopping multiple access (THMA) is selected in this research as the multi user access format with which different TH codes are allocated to different UWB users and each UWB user is exploiting orthogonality of different TH code to reduce the multiple access interference (MAI) at the receiver[19]. Due to this characteristic, each UWB user is not required to be synchronized with the network coordinator (NC) before it can start data transmission. However, in the asynchronous transmission mode, the user n may transmit its own data frame with an individual relative time offset δ_n . In addition, each transmission signal is subjects to multipath effects of the radio channel. Thus, MAI cannot be completely eliminated at the receiver. Therefore, transmission power of each UWB user is considered as the essential factor to influence the overall throughput of the UWB network. Without coordinated power allocation scheme, each user may decide to use the maximal transmission power within the FCC limits to enhance its own link quality. However, maximum transmission power of each user will lead to high energy consumption and high MAI to other users and degrade the QoS in the UWB network. Therefore, an OPA will be considered which yields better performance than the MPA. The NC is responsible to allocate each active UWB user a TH code and estimate the channel state information (CSI) and path loss parameters. Then OPA module deployed on the NC shall be executed to allocate optimal transmission power to each UWB user according to these parameters.

The OPA algorithm is described in section 5.4. The system model and transceivers are described in sections 5.2 and 5.3, including the impulse radio in 5.2, the rake receiver in 5.3.2 and the SML receiver in 5.3.3. Simulation results are presented in section 5.5. Section 6 concludes this chapter.

5.2 System model and network structure

An UWB network with a set of N nodes is considered. For simplicity, it assumes that the UWB network contains only one location fixed network coordinator (NC), serving as the administration node for the N UWB nodes. The N UWB nodes are uniformly distributed over the area F .

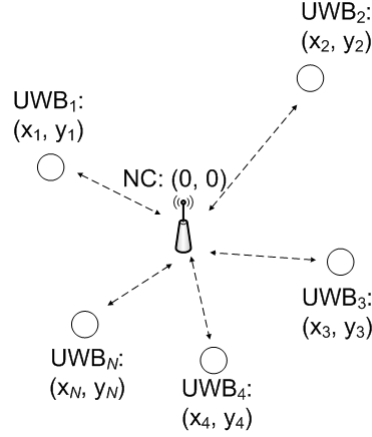


Figure 11: Centralized UWB network structure

Figure 11 illustrates the centralized UWB network structure. The NC is fixed at coordinates $(x_{NC}, y_{NC}) = (0, 0)$, whereas the N UWB nodes move over time and their locations are uniformly distributed over F . The demands for communication are always from the UWB users to the NC. In this research, only the uplink transmission is considered. A communication scheme as specified in IEEE 802.15a shall be considered [20]. As multiple access schemes a pseudo random time hopping code is allocated to each active UWB user to lower the probability of repeated pulse collision from two users. Binary pulse position modulation (2-PPM) is assumed as modulation scheme for all UWB users. The transmitted signal of the user n can then be written as

$$s_n(t) = A_n \sum_{k=-\infty}^{+\infty} \sum_{j=1}^{N_s} g(t - kT_s - jT_f - c_{j,n}T_c - a_{k,n}\varepsilon - \delta_n), \quad n = 1, 2, \dots, N, \quad (47)$$

where A_n is the amplitude of the transmitted pulse, $g(t)$ is the normalized transmitted pulse which adheres to the specification 802.15.4a [20], T_s is the symbol duration, T_f is the pulse repetition time interval, T_c is the chip duration, $a_{k,n}$ is the k -th information bit of the n -th user, ε is the pulse position modulation (PPM) offset and N_s is the number of pulse repetition period. It can be seen from equation (27), each information bit is transmitted by N_s identical pulses to enhance quality of reception and the n -th user starts its transmission with the time offset δ_n , which is assumed to be uniformly distributed over the time $[0, T_s]$.

5.3 Multi user receivers

5.3.1 Fundamentals

Each user n transmits its modulated UWB signal through a multipath channel with channel impulse response

$$\underline{h}_n(\tau, t) = \sum_{l=1}^L h_{l,n}(t) \Delta(\tau - \tau_{l,n}(t)) = \sum_{l=1}^L a_l(t) e^{i\theta_l(t)} \Delta(\tau - \tau_{l,n}(t)), \quad n = 1, 2, \dots, N. \quad (48)$$

where $\Delta(\tau)$ is the Dirac delta function. We assume that the amplitude $a_l(t)$ and the phase $\theta_l(t)$ of each tap keep unchanged during each frame transmission due to the weak Doppler effect in the indoor environment [21]. The equation can be rewritten as

$$\underline{h}_n(\tau) = \sum_{l=1}^L h_{l,n} \Delta(\tau - \tau_{l,n}), \quad n = 1, 2, \dots, N, \quad (49)$$

where L is the number of paths of $h_n(\tau)$, $a_{l,n}$, $\theta_{l,n}$ and $\tau_{l,n}$ are amplitude, phase and the delay of the l -th path, respectively. Hence, the received signal for user n can be expressed as

$$r_n(t) = s_n(t) \otimes \underline{h}_n(t) = A_n \sum_{k=-\infty}^{+\infty} \sum_{j=1}^{N_s} \sum_{l=1}^L h_{l,n} g(t - \tau_{l,n} - kT_s - jT_f - c_{j,n}T_c - a_{k,n}\varepsilon - \delta_n). \quad (50)$$

where “ \otimes ” represents the Kronecker operation and $g(t)$ is the transmitted pulse. Thus, the combined received signal from N UWB users can be expressed as

$$r(t) = \sum_{n=1}^N r_n(t) + n(t), \quad (51)$$

where $n(t)$ is the additive white Gaussian noise (AWGN) with power spectral density (PSD) N_0 .

5.3.2 Multiuser rake receiver

Assuming perfect channel estimation, the matched signal $v_n(t)$ of the n -th receiver becomes (cf. [19])

$$v_n(t) = \sum_{j=1}^{N_s} g(t - jT_f - c_{j,n}T_c) - \sum_{j=1}^{N_s} g(t - jT_f - c_{j,n}T_c - \varepsilon). \quad (52)$$

The M -finger multi user rake receiver uses $v_n(t)$ to correlate the combined received signal $r(t)$ [19]. It gets

$$z_{k,n} = \sum_{l=1}^M \int_{(k-1)T_s}^{kT_s} h_{l,n}^* r(t) v_n(t - \tau_{m,n}) dt, \quad (53)$$

where $h_{l,n}^*$ is the complex conjugate of $h_{l,n}$ and $z_{k,n}$ is the k -th correlation result of n -th user [19]. Then the information bit can be estimated through

$$a_{k,n} = \begin{cases} 0 & \text{Re}\{z_{k,n}\} > 0 \\ 1 & \text{Re}\{z_{k,n}\} < 0 \end{cases}, \quad n = 1, 2, \dots, N. \quad (54)$$

and $z_{k,n}$ may be a complex number due to two reasons:

1. The integral time length is T_s is smaller than the received symbol duration due to the time delay of multi path channel.
2. The number M of fingers may be smaller than the number L of channel paths.

It is obvious that $z_{k,n}$ may contain MAI due to the possible pulses overlap among the N users. We define that $I_{m,n}$ is the interference from m -th user to n -th user. Since each UWB user starts its transmission at arbitrary time point, each interferer m of the n -th user transmits its frame with a relative time offset δ_m , which is uniformly distributed over the time $[0, T_s]$. The transmission power and path gain of each UWB user can be expressed as

$$\mathbf{p}_{\text{tx}} = [p_{1,\text{tx}} \quad p_{2,\text{tx}} \quad \cdots \quad p_{N,\text{tx}}]^T \quad (55)$$

and

$$\mathbf{g} = [g_1 \quad g_2 \quad \cdots \quad g_N]. \quad (56)$$

Hence, \underline{I}_{mn} can be calculated as

$$\underline{I}_{mn} = \frac{1}{T_s} \int_0^{T_s} \left[\int_0^{T_s} \sum_{l=1}^M h_{l,n}^* r_m'(t-\delta) v_n(t-\tau_{l,n}) dt \right]^2 d\delta, \quad (57)$$

where T_s is the symbol duration and

$$r_m'(t) = A_m \sum_{l=1}^L \left(h_{l,m} \sum_{j=1}^{N_s} g(t - jT_f - c_{j,m}T_c - \tau_{l,m}) \right), \quad (58)$$

with the amplitude A_m of the transmitted pulse of the m -th user, which has power

$$p_{m,\text{tx}} = A_m^2, \quad (59)$$

due to the extreme short pulse duration. We set

$$\sigma_{mn}(\delta) = \int_0^{T_s} \left(\sum_{j=1}^{N_s} g(t - jT_f - c_{j,m}T_c - \delta) \right) v_n(t) dt, \quad (60)$$

where δ denotes the time offset. The equation (57) can be approximated as

$$\underline{I}_{mn} \approx \left(\frac{A_m}{T_s} \sum_{l=1}^M (h_{l,n}^* h_{l,m}) \int_0^{T_s} \sigma_{mn}(\delta) d\delta \right)^2 = \frac{p_{m,\text{tx}}}{T_s^2} \left(\sum_{l=1}^M (h_{l,n}^* h_{l,m}) \right)^2 \left(\int_0^{T_s} \sigma_{mn}(\delta) d\delta \right)^2. \quad (61)$$

For the n -th user, the sum of interference can be expressed as

$$\underline{I}_n = \sum_{m=1, m \neq n}^N \underline{I}_{mn}, \quad n = 1, 2, \dots, N. \quad (62)$$

According to Cauchy–Schwarz inequality

$$\underline{I}_{mn} \leq \frac{1}{T_s} \int_0^{T_s} \left[\int_0^{T_s} (r_m'(t-\delta))^2 dt \right] \left[\int_0^{T_s} \left(\sum_{l=1}^M h_{l,n}^* v_n(t-\tau_{l,n}) \right)^2 dt \right] d\delta. \quad (63)$$

Since the monocycles appearing in $s_n(t)$ are widely separated from each other, even a small time misalignment makes virtually orthogonal. The equation can be written as

$$\begin{aligned}
I_{mn} &\leq \frac{1}{T_s} \int_0^{T_s} \left[\left(|A_m|^2 \sum_{l=1}^L N_s |h_{l,m}|^2 \right) \left(2 \sum_{l=1}^M N_s |h_{l,n}^*|^2 \right) \right] d\delta \\
&= \frac{2 p_{m,\text{tx}} N_s^2}{T_s} \int_0^{T_s} \left(\sum_{l=1}^L |h_{l,m}|^2 \sum_{l=1}^M |h_{l,n}^*|^2 \right) d\delta \\
&= 2 p_{m,\text{tx}} N_s^2 \sum_{l=1}^L |h_{l,m}|^2 \sum_{l=1}^M |h_{l,n}^*|^2
\end{aligned} \tag{64}$$

The useful signal energy E_b can be expressed as

$$E_{b,n} = \left(\int_0^{T_s} \sum_{l=1}^M h_{l,n}^* r_n'(t) v_n(t - \tau_{l,n}) dt \right)^2, \tag{65}$$

where

$$r_n'(t) = A_n \sum_{l=1}^L \left(h_{l,n} \sum_{j=1}^{N_s} g(t - jT_f - c_{j,n}T_c - \tau_{l,n}) \right). \tag{66}$$

And it can be expressed as

$$\begin{aligned}
E_{b,n} &= \left(\int_0^{T_s} \sum_{l_{\text{rx}}=1}^M h_{l_{\text{rx},n}}^* A_n \sum_{l_{\text{tx}}=1}^L h_{l_{\text{tx},n}} \sum_{j=1}^{N_s} g(t - jT_f - c_{j,n}T_c - \tau_{l_{\text{tx},n}}) v_n(t - \tau_{l_{\text{rx},n}}) dt \right)^2 \\
&\approx \left(A_n N_s \sum_{l=1}^M |h_{l,n}|^2 \right)^2 = p_{n,\text{tx}} N_s^2 \left(\sum_{l=1}^M |h_{l,n}|^2 \right)^2
\end{aligned} \tag{67}$$

Hence, the signal to interference and noise ratio (SINR) at the receiver for user n can be written as

$$\gamma_n = \frac{E_{b,n}}{N_0' + I_n}, \quad n = 1, 2, \dots, N. \tag{68}$$

where I_n is from previous definition and considered as the additive white Gaussian noise (AWGN) at the receiver and $N_0' = N_s N_0$ [19]. Hence, the bit error ratio (BER) of the multi user rake receiver can be expressed as [19]

$$P_{b,n} = \frac{1}{2} \operatorname{erfc} \left(\sqrt{\frac{\gamma_n}{2}} \right). \tag{69}$$

5.3.3 Successive maximum likelihood receiver

Let

$$\underline{h}_n = [h_{1,n} \quad h_{2,n} \quad \dots \quad h_{L,n}] \tag{70}$$

be the vector of the L_n first taps of the discrete complex channel impulse response of the n -th user, which covers 85% of the whole channel energy. The sampling rate is $2/T_c$ and we set

$$T_c = \delta + T_p. \tag{71}$$

where T_p is the pulse duration and $\delta = T_p$.

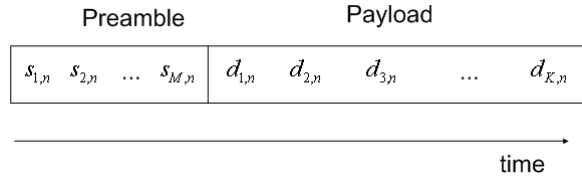


Figure 12: Structure of transmitted frame

Figure 12 shows the frame structure. Each transmitted frame consists of two parts: preamble and payload. The preambles are known by the receiver while the information bits are contained in the payload. Before transmission, each user shall be allocated a different preamble sequence s_n by the NC, which shall be spread by the delta function δ_L according to [20], which can be expressed as

$$\delta_{L_p} = \underbrace{[1 \ 0 \ \dots \ 0]}_{L_p}. \quad (72)$$

Hence, the spread preamble sequence can be expressed as

$$\begin{aligned} \mathbf{s}_n^s &= [s_{1,n} \otimes \delta_{L_p} \quad s_{2,n} \otimes \delta_{L_p} \quad \dots \quad s_{M,n} \otimes \delta_{L_p}] \\ &= [g_{1,n} \quad g_{2,n} \quad \dots \quad g_{ML_p,n}] \end{aligned} \quad (73)$$

with “ \otimes ” being the Kronecker operation [4]. Each data symbol of the n -th user shall be spread by the time hopping code \mathbf{c}_n , which can be expressed as a vector with length of L_c (cf. [20]):

$$\mathbf{c}_n = \underbrace{[0 \ 0 \ 1 \ \dots \ 0]}_1 \dots \underbrace{[0 \ 1 \ 0 \ \dots \ 0]}_{N_{\text{Burst}}}. \quad (74)$$

It can be seen the position of “1” in each burst can be determined by the value of the allocated time hopping code. The k -th transmitted bit of the n -th user shall be modulated through \mathbf{c}_n and the time offset vector $\boldsymbol{\sigma}_i$ (cf. [19]),

$$\boldsymbol{\sigma}_k = \begin{cases} [1 \ 0], & d_{k,n} = 0 \\ [0 \ 1], & d_{k,n} = 1 \end{cases}. \quad (75)$$

The k -th spread transmitted bit of the n -th user can be expressed as a vector with the length of $2L_c$

$$\mathbf{d}_{k,n}^s = A_n \mathbf{c}_n \otimes \boldsymbol{\sigma}_k, \quad (76)$$

where A_n is the amplitude of the transmitted pulses. For each transmitted bit k , we set the discrete complex channel of the n -th user in a Toeplitz matrix form $\underline{\mathbf{H}}_{k,n}$,

$$\underline{\mathbf{H}}_{k,n} = \underbrace{\begin{bmatrix} \underline{h}_{1,n} & 0 & \cdots & 0 \\ \underline{h}_{2,n} & \underline{h}_{1,n} & \cdots & 0 \\ \vdots & \underline{h}_{2,n} & \cdots & 0 \\ \underline{h}_{L_n,n} & \vdots & \cdots & 0 \\ 0 & \underline{h}_{L_n,n} & \ddots & \underline{h}_{1,n} \\ 0 & 0 & \ddots & \underline{h}_{2,n} \\ 0 & 0 & \cdots & \vdots \\ 0 & 0 & \cdots & \underline{h}_{L_n,n} \end{bmatrix}}_{2L_c}, \quad (77)$$

which has (L_n+2L_c-1) rows and $2L_c$ columns. The original k -th received data vector of the n -th user with the length of (L_n+2L_c-1) can be expressed as

$$\underline{\mathbf{r}}_{k,n} = \underline{\mathbf{H}}_{k,n} \mathbf{d}_{k,n}^s + \underline{\mathbf{n}}_{k,n}, \quad k=1,2,\dots,K, \quad n=1,2,\dots,N. \quad (78)$$

Setting

$$L_r = L_n + 2L_c - 1 \quad (79)$$

yields

$$K_{\text{ISI}} = \left\lfloor \frac{L_r}{2L_c} \right\rfloor - 1, \quad (80)$$

which is the number of data symbols that are subjected to the inter symbol interference (ISI) from the current symbol k due to the multipath effect. $\underline{\mathbf{H}}_{k,n}$ can be rewritten as

$$\underline{\mathbf{H}}_{k,n} = \begin{bmatrix} \underline{\mathbf{H}}_{k,n}^{(1)} \\ \underline{\mathbf{H}}_{k,n}^{(2)} \\ \vdots \\ \underline{\mathbf{H}}_{k,n}^{(1+K_{\text{ISI}})} \end{bmatrix}, \quad (81)$$

where each sub matrix $\underline{\mathbf{H}}_{k,n}^{(i)}, i=1,2,\dots,K_{\text{ISI}}$ has $2L_c$ rows and $2L_c$ columns, whereas $\underline{\mathbf{H}}_{k,n}^{(1+K_{\text{ISI}})}$ has $(L_r-2K_{\text{ISI}}L_c)$ rows and $2L_c$ columns. The received data vector of the n -th user can be written as

$$\underline{\mathbf{r}}_n = \begin{bmatrix} \underline{\mathbf{r}}_n^{(1)} \\ \underline{\mathbf{r}}_n^{(2)} \\ \vdots \\ \underline{\mathbf{r}}_n^{(K)} \end{bmatrix} = \underline{\mathbf{H}}_n \begin{bmatrix} \underline{\mathbf{d}}_{1,n}^s \\ \underline{\mathbf{d}}_{2,n}^s \\ \vdots \\ \underline{\mathbf{d}}_{K,n}^s \end{bmatrix} + \underline{\mathbf{n}}_n, \quad (82)$$

with the system matrix

$$\underline{\mathbf{H}}_n = \underbrace{\begin{bmatrix} \underline{h}_{1,n} & 0 & \cdots & 0 \\ \underline{h}_{2,n} & \underline{h}_{1,n} & \cdots & 0 \\ \vdots & \underline{h}_{2,n} & \cdots & 0 \\ \underline{h}_{L_n,n} & \vdots & \cdots & 0 \\ 0 & \underline{h}_{L_n,n} & \ddots & \underline{h}_{1,n} \\ 0 & 0 & \ddots & \underline{h}_{2,n} \\ 0 & 0 & \cdots & \vdots \\ 0 & 0 & \cdots & \underline{h}_{L_n,n} \end{bmatrix}}_{2KL_c}. \quad (83)$$

The observed data vector at the receiver can be expressed as

$$\underline{\mathbf{r}} = \sum_{n=1}^N \underline{\mathbf{r}}_n = \begin{bmatrix} \underline{\mathbf{r}}^{(1)} \\ \underline{\mathbf{r}}^{(2)} \\ \vdots \\ \underline{\mathbf{r}}^{(K)} \end{bmatrix}. \quad (84)$$

We get

$$\begin{aligned} \underline{\mathbf{d}}_{k,n}^{s,0} &= A_n \underline{\mathbf{c}}_n \otimes [1 \ 0], \\ \underline{\mathbf{d}}_{k,n}^{s,1} &= A_n \underline{\mathbf{c}}_n \otimes [0 \ 1], \\ \underline{\mathbf{z}}_{k,n}^0 &= \underline{\mathbf{H}}_{k,n}^{(1)} \underline{\mathbf{d}}_{k,n}^{s,0} + \sum_{i=1}^{K_{\text{ISI}}} \underline{\mathbf{H}}_{k-i,n}^{(i+1)} \underline{\mathbf{d}}_{k-i,n}^s, \\ \underline{\mathbf{z}}_{k,n}^1 &= \underline{\mathbf{H}}_{k,n}^{(1)} \underline{\mathbf{d}}_{k,n}^{s,1} + \sum_{i=1}^{K_{\text{ISI}}} \underline{\mathbf{H}}_{k-i,n}^{(i+1)} \underline{\mathbf{d}}_{k-i,n}^s, \\ \underline{\mathbf{d}}_{k,n} &= \arg \min_m \left(\left\| \underline{\mathbf{z}}_{k,n}^m - \underline{\mathbf{r}}^{(k)} \right\| \right), m = 0, 1. \end{aligned} \quad (85)$$

5.4 Optimal power allocator

5.4.1 Fundamentals

In this research, the Optimal Power Allocator (OPA) is only investigated with the multi user rake receiver. The bit error probability $P_{b,n}$ can be calculated as

$$P_{b,n} = \frac{1}{2} \operatorname{erfc} \left(\sqrt{\frac{1}{2} \frac{p_{n,\text{tx}} N_s^2 \left(\sum_{l=1}^M |\underline{h}_{l,n}|^2 \right)^2}{N_s N_0 + \sum_{m=1, m \neq n}^N \left(\frac{p_{m,\text{tx}}}{T_s^2} \left(\sum_{l=1}^M (h_{l,n}^* h_{l,m}) \right)^2 \left(\int_0^{T_s} \sigma_{mn}(\delta) d\delta \right)^2 \right)}}} \right). \quad (86)$$

It assumes that each user transmits M data bits and D is the overall transmission duration that is from transmission beginning of the first user to transmission end of the last user. Hence, the overall throughput can be expressed as (cf. [21])

$$T_{\text{sum}}(\mathbf{p}) = \frac{1}{D} \sum_{n=1}^N M(1 - P_{b,n}(\mathbf{p})), \quad (87)$$

where

$$\mathbf{p} = [p_{1,\text{tx}} \quad p_{2,\text{tx}} \quad \cdots \quad p_{N,\text{tx}}]^T. \quad (88)$$

After optimal power allocation (OPA), the optimal power vector \mathbf{p}_{opt} shall be achieved to

$$\begin{aligned} \mathbf{p}_{\text{opt}} &= \arg \max_{\mathbf{p}} (T_{\text{sum}}(\mathbf{p})) \\ &= \arg \max_{\mathbf{p}} \left(\sum_{n=1}^N (1 - P_{b,n}(\mathbf{p})) \right). \end{aligned} \quad (89)$$

The procedure of finding \mathbf{p}_{opt} is described in section 5.4.2.

5.4.2 Determine the Minimum Transmission Power of each User

The transmission power of each user shall be larger than a minimum value to guaranty its own link quality. It assumes that the minimal SINR of the n -th user is $\gamma_{n,\text{min}}$ (dB) according to its different service type. We set the unit power interference I_{mn}^u as

$$I_{mn}^u = \frac{I_{mn}}{p_{m,\text{tx}}} = \frac{1}{T_s^2} \left(\sum_{l=1}^M (h_{l,n}^* h_{l,m}) \right)^2 \left(\int_0^{T_s} \sigma_{mn}(\delta) d\delta \right)^2, \quad n=1,2,\dots,N, \quad m=1,2,\dots,N, \quad m \neq n. \quad (90)$$

The requirement of the minimal SINR $\gamma_{n,\text{min}}$ yields

$$\frac{p_{n,\text{tx}} N_s^2 \left(\sum_{l=1}^M |h_{l,n}|^2 \right)}{N_s N_0 + \sum_{m=1, m \neq n}^N p_{m,\text{tx}} I_{mn}^u} \geq 10^{\frac{\gamma_{n,\text{min}}}{10}}, \quad n=1,2,\dots,N. \quad (91)$$

Then it can be rewritten as

$$\mathbf{Gp} \geq \mathbf{n}'. \quad (92)$$

where

$$\mathbf{G} = \begin{bmatrix} N_s^2 \left(\sum_{l=1}^M |h_{l,1}|^2 \right) & -10^{\frac{\gamma_{1,\text{min}}}{10}} I_{21}^u & \cdots & -10^{\frac{\gamma_{1,\text{min}}}{10}} I_{N1}^u \\ -10^{\frac{\gamma_{2,\text{min}}}{10}} I_{12}^u & N_s^2 \left(\sum_{l=1}^M |h_{l,2}|^2 \right) & \cdots & -10^{\frac{\gamma_{2,\text{min}}}{10}} I_{N2}^u \\ \vdots & \vdots & \ddots & \vdots \\ -10^{\frac{\gamma_{N,\text{min}}}{10}} I_{1N}^u & -10^{\frac{\gamma_{N,\text{min}}}{10}} I_{2N}^u & \cdots & N_s^2 \left(\sum_{l=1}^M |h_{l,N}|^2 \right) \end{bmatrix} \quad (93)$$

$$\mathbf{n}' = \left[10^{\frac{\gamma_{1,\min}}{10}} N_s N_0 \quad 10^{\frac{\gamma_{2,\min}}{10}} N_s N_0 \quad \dots \quad 10^{\frac{\gamma_{N,\min}}{10}} N_s N_0 \right]^T. \quad (94)$$

\mathbf{G} is a positive definite matrix if I_{mn}^u is smaller enough than N_s^2 . Then

$$\mathbf{p} \geq \mathbf{p}_{\min} = \mathbf{G}^{-1} \mathbf{n}'. \quad (95)$$

5.4.3 Find the optimum transmission power of each user iteratively

The maximum transmission power of each user is p_{\max} , which adheres to the Federal Communications Commission (FCC) requirement [20]. Our task is to find the optimum power vector, which is a nonlinear optimization problem. Computation of the gradient function and Hessian matrix of $T_{\text{sum}}(\mathbf{p})$ has a high complexity with the increase of number of users N . Therefore, an iterative algorithm shall be used to find a local maximum value of $T_{\text{sum}}(\mathbf{p})$. The pseudo code of the algorithm can be expressed as:

```

 $p_{n,\text{ini}} = p_{\max}, n = 1, 2, \dots, N;$ 
 $p_n = [p_{n,\text{min}}, p_{\max}, C], n = 1, 2, \dots, N;$  //power candidate vector. C:
number of elements
for  $\text{cnt\_L} = 1$  to  $N_{\text{Loops}}$ 
   $T_{\text{cnt\_n},\text{cnt\_p}} = 0;$ 
  for  $\text{cnt\_n} = 1$  to  $N$ 
    for  $\text{cnt\_p} = 1$  to  $C$ 
       $T_{\text{cnt\_n},\text{cnt\_p}} = T_{\text{sum}}\{p_{\text{cnt\_n}}(\text{cnt\_p}), (p_{n,\text{ini}}, n \neq \text{cnt\_n})\};$ 
    end
     $p_{\text{cnt\_n},\text{ini}} = \text{argmax}(T_{\text{cnt\_n},\text{cnt\_p}});$ 
  end

```

5.4.4 Computational complexity of optimal power allocation

The computational complexity of the optimal power allocation (OPA) is

$$O(\text{OPA}) = N_{\text{loops}} N C. \quad (96)$$

where N_{loops} is the number of loops, N is the number of active users and C is the length of the candidate power vector.

5.5 Simulation results

The performance simulation results of the 22-finger rake receiver and SML receiver are depicted in Figure 13. For simplicity, only single user scenario is investigated, MAI from interferers are considered as AWGN. Particularly for high SNR, the SML achieves much lower BER than the rake receiver.

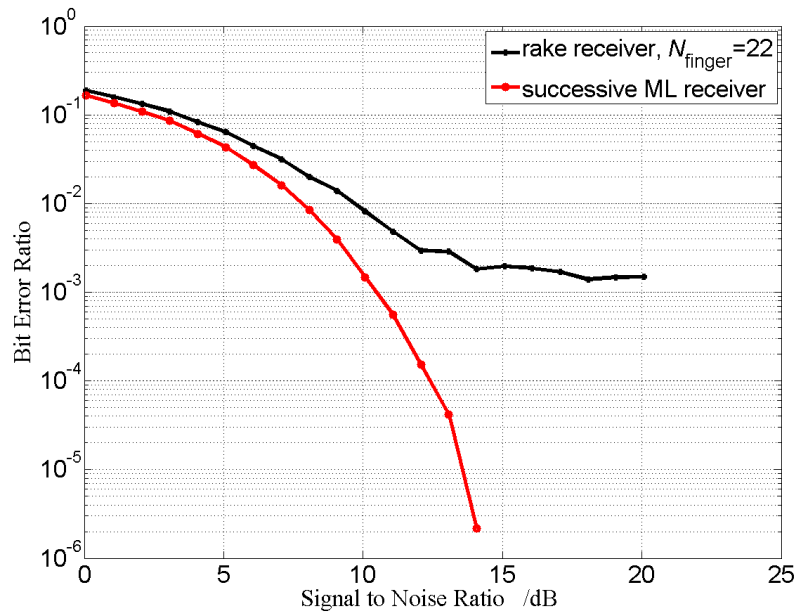


Figure 13: Bit error ratio of the 22-finger rake receiver and the SML receiver

Figure 14 shows the overall throughput with increasing number of active users using multi user rake receiver. OPA outperforms MPA, when the number of active users increases.

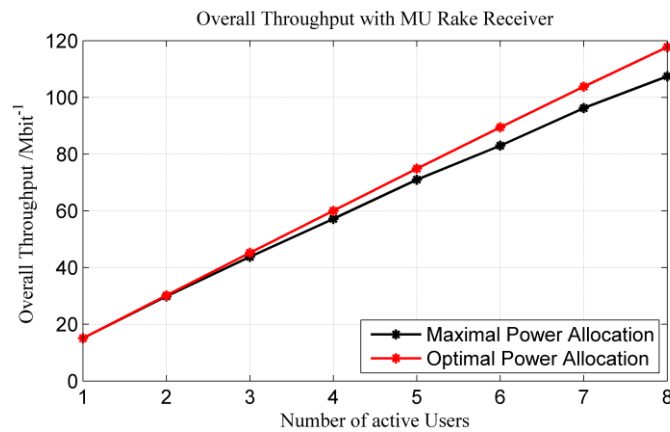


Figure 14: Overall throughput of OPA and MPA for different number of active users

6 Conclusion

In this research an optimal power allocation (OPA) mechanism has been applied to a centralized UWB network. In contrast to conventional maximum power allocation (MPA) schemes, the OPA requires the knowledge of the interference situation at every UWB user. Simulation results show that this knowledge can be used to increase the overall network throughput. The here utilized simulation system framework, include a UWB multipath channel. Furthermore a rake receiver and a SML receiver have been applied.

7 Appendix

7.1 Annex 1

By expanding the definition (21) we can write:

$$MSE = \frac{1}{E_x} \left[\mathbb{E} \int_{\mathfrak{R}^l} \{\hat{X}^2(s) ds\} + \int_{\mathfrak{R}^l} x^2(s) ds - 2 \mathbb{E} \int_{\mathfrak{R}^l} \{\hat{X}^2(s) x(s) ds\} \right] \quad (97)$$

The first term in (27) using the Parseval's relationship and considering that $\int_{\mathfrak{R}^l} E_x(\nu) d\nu = E_x$ is

$$\begin{aligned} \frac{1}{E_x} \int_{\mathfrak{R}^l} \mathbb{E} \{\hat{X}^2(s)\} ds &= \frac{1}{E_x} \int_{\mathfrak{R}^l} |\Phi(\nu)|^2 \mathfrak{F}^{(l)}[\mathbb{E}\{Y(s)Y(s-\tau)\}] d\nu \\ &= \frac{1}{E_x} \int_{\mathfrak{R}^l} |\Phi(\nu)|^2 \bar{E}_H(\nu) d\nu + \frac{1}{E_x} \int_{\mathfrak{R}^l} |\Phi(\nu)|^2 \bar{E}_W(\nu) d\nu \end{aligned} \quad (98)$$

Now the autocorrelation function of the process $W(s)$ may be written as

$$\begin{aligned} \bar{R}_W(\tau) &= \int_{\mathfrak{R}^l} \mathbb{E}\{W(s)W(s-\tau)\} ds \\ &= \mathbb{E} \left\{ \sum_{k=1}^K \sum_{h=1}^K w_k w_h \int_{\mathfrak{R}^l} \delta(s-s_k) \delta(s-\tau-s_h) ds \right\} \\ &= \delta(\tau) \mathbb{E} \left\{ \sum_{k=1}^K \sigma_k^2 \right\}. \end{aligned} \quad (99)$$

where we have used the property that w_k 's are independent and the last expectation is taken with respect to RV K . Hence, the energy spectral density is

$$\bar{E}_W(\nu) = \mathfrak{F}^{(l)}[\bar{R}_W(\tau)] = \mathbb{E} \left\{ \sum_{k=1}^K \sigma_k^2 \right\}. \quad (100)$$

By substituting (30) into (28) we get

$$\begin{aligned} \frac{1}{E_x} \int_{\mathfrak{R}^l} \mathbb{E} \{\hat{X}^2(s)\} ds &= 1 + \frac{\beta}{\rho} + \frac{1}{E_x} \mathbb{E} \left\{ \sum_{k=1}^K \sigma_k^2 \right\} \int_{\mathfrak{R}^l} |\Phi(\nu)|^2 d\nu \\ &= 1 + \frac{\beta}{\rho} + \frac{\beta}{\rho^2} \mathbb{E} \left\{ \sum_k \frac{\sigma_k^2}{E_x} \right\} = 1 + \frac{\beta}{\rho} + \frac{\beta}{\rho^2} \bar{l} \end{aligned} \quad (101)$$

where we recalled the definition of \bar{D} in (10).

The second term is equal to 1 whereas the third term is given by

$$-\frac{2}{E_x} \int_{\mathfrak{R}^d} \mathbf{E}\{\hat{X}(s)\} \cdot x(s) ds = -\frac{2}{E_x} \int_{\mathfrak{R}^d} \Phi(\nu) \mathbf{E}\{S_Y(\nu)\} S_x^*(\nu) d\nu \quad (102)$$

where $S_Y(\nu) = \mathfrak{F}^{(l)}[Y(s)]$. Due to the stationarity of the random process $P(s)$ and considering that $\mathbf{E}\{w_k\} = 0$ it is

$$\mathbf{E}\{S_Y(\nu)\} = \mathbf{E}\{\mathfrak{F}^{(l)}[x(s) \cdot P(s)]\} = \mu_p \cdot S_x(\nu). \quad (103)$$

By substitution of (32), (31) becomes

$$-\frac{2}{E_x} \int_{\mathfrak{R}^d} \mathbf{E}\{\hat{X}(s)\} \cdot x(s) ds = -\frac{2}{E_x} \rho \int_{\mathfrak{R}^d} \Phi(\nu) \bar{E}_x(\nu) d\nu = -2. \quad (104)$$

8 References

- [1] R. Verdone, D. Dardari, G. Mazzini, A. Conti, "Wireless Sensor and Actuator Networks: Technologies, Analysis and Design," Elsevier, London, UK, 2008.
- [2] Tony Q.S. Quek, Davide Dardari, and Moe Z. Win, "Energy Efficiency of Dense Wireless Sensor Networks: To Cooperate or Not to Cooperate," IEEE Journal on Selected Areas in Communication (Special Issue on Cooperative Communications and Networking), Vol. 25, No. 2, Feb. 2007.
- [3] D. Dardari, A. Conti, C. Buratti and R. Verdone, "Mathematical Evaluation of Environmental Monitoring Estimation Error through Energy-Efficient Wireless Sensor Networks," Mobile Computing, IEEE Transactions on , vol.6, no.7, pp.790-802, July 2007.
- [4] N. Wernersson, J. Karlsson and M. Skoglund, "Distributed quantization over noisy channels," IEEE Transactions on Communications, Volume 57, Issue 6, June 2009 Page(s):1693 - 1700.
- [5] A. Oka and L. Lampe, "Incremental distributed identification of Markov random field models in wireless sensor networks," IEEE Transactions on Signal Processing, Volume 57, Issue 6, June 2009 Page(s):2396 - 2405.
- [6] A. Ribeiro and G. Giannakis, "Bandwidth-Constrained Distributed Estimation for Wireless Sensor Networks - Part I: Gaussian Case," IEEE Transactions on Signal Processing, Volume 54, Issue 3, March 2006 Page(s):1131 - 1143.
- [7] J.-J. Xiao, S. Cui, Z.-Q. Luo and A. J. Goldsmith, "Joint Estimation in Sensor Networks under Energy Constraints," IEEE Trans. on Signal Processing, 2005.
- [8] Matamoros, J.; Anton-Haro, C., "Bandwidth Constraints in Wireless Sensor-Based Decentralized Estimation Schemes for Gaussian Channels," Global Telecommunications Conference, 2008. IEEE GLOBECOM 2008. IEEE pp.1-5, Nov. 30 2008-Dec. 4 2008.
- [9] H. Zhang, J. M. F. Moura and B. Krogh, "Dynamic Field Estimation Using Wireless Sensor Networks: Tradeoffs Between Estimation Error and Communication Cost," IEEE Transactions on Signal Processing, Volume 57, Issue 6, June 2009 Page(s):2383 - 2395.
- [10] M. C. Vuran, O. B. Akan, and I. F. Akyildiz, "Spatio-temporal correlation: theory and applications for wireless sensor networks," Comput. Netw. J., vol. 45, no. 3, pp. 245-261, Jun. 2004.
- [11] W.A. Gardner, "Introduction to random processes: with applications to signals and systems," McGraw Hill, second edition, 1989.
- [12] E. Masry, "Poisson sampling and spectral estimation of continuous-time processes," IEEE Trans. on Inf. Theory, vol. IT-24, no.2, March 1978, pp. 173-183.
- [13] F. Marvasti, "Signal recovery from nonuniform samples and spectral analysis on random nonuniform samples," IEEE International Conference on Acoustics, Speech, and Signal Processing, ICASSP '86, Volume: 11, Apr 1986, pp. 1649-1652.
- [14] D. Dardari and F. Fabbri, "Spatial field estimation through wireless sensor networks under bandwidth constraints," in IEEE Global Communications Conference (GLOBECOM 2010), Miami, Florida, USA, dec 2010, pp. 1-5.
- [15] J. Matamoros, F. Fabbri, C. Anton-Haro, and D. Dardari, "On the estimation of randomly sampled 2D spatial fields under bandwidth constraints," accepted for publication on IEEE Trans. Wireless Commun., 2011.
- [16] Abdelaziz Bouzegzi and all, "A second order statistics based algorithm for blind recognition of OFDM based systems", Globecom, 2008
- [17] Zeisberg, S., Schreiber, V.: "EUWB - Coexisting Short Range Radio by Advanced Ultra-Wideband RadioTechnology", ICT Mobile and Wireless Communications Summit, Stockholm, June 2008, accepted for publication
- [18] URL of EUWB consortium: <http://www.euwb.eu>

- [19] Benedetto, M.; Giancola, G., "Understanding Ultra Wide Band Radio Fundamentals," Prentice Hall Communications Engineering and Emerging Technologies Series, 2004.
- [20] IEEE Standard 802.15.4a, "Wireless Medium Access Control (MAC) and Physical Layer (PHY) Specifications for Low-Rate Wireless Personal Area Networks (WPANs)," 2007.
- [21] Tse, D.; Viswanath, P., "Fundamentals of Wireless Communication," Cambridge University Press, 2005.
- [22] S. O. Rice, "Mathematical analysis of random noise," Bell Syst. Tech. J., vol. 23, pp. 46–156, Jan. 1945.
- [23] M. Gudmundson, "Correlation model for shadowing fading in mobile radio systems," Electron. Lett., vol. 27, pp. 2145–2146, Nov. 1991.
- [24] J.B. Pred and all, "Distributed learning in wireless sensor networks", IEEE Signal Processing Mag., V23, #4, pp. 56-69, 2006.
- [25] N. Aronszajn, "Theory of reproducing kernels", Tr. Of the mathematical society, V68, #3, pp. 337-404, may 1950.
- [26] B. Schölkopf and all, "A generalized representer theorem", Royal Holloway College, Univ. London, UK, Tech, Rep. NC2-TR-2000-81, 2000
- [27] C. Richard and al., "Online prediction of time series data with kernels", IEEE Tr. On signal processing, V57, #3, march 2009.
- [28] T. Poggio and F. Girosi, "Notes on PCA, regularization, sparsity and support vector machines", Rep. MIT artificial intelligence lab., may 1998.
- [29] A. Rakotomamonjy and S. Canu, "Frame, Reproducing kernel, regularization and learning", Rep. INSA de Rouen (France), 2001
- [30] P.Honeine and all, "Functional estimation in Hilbert space for distributed learning in wireless sensor networks", IEEE ICASSP 2009.
- [31] D. Kotzor and W. Utschick, "A kernel approach for estimating the position of moving objects", IEEE ICASSP, 2010.L. Csato and M. Opper, "Sparse representation for gaussian process models", Adv. in neural inf. Processing Systems, MIT Press, pp. 444-450, 2001.
- [32] D.L. Donoho, "Compressed sensing", IEEE Tr. Information theory, V52, #4, pp. 1289-1306, 2006.
- [33] P. Honeine and all, "On line non linear sparse approximation of functions", IEEE Proc. Of ISIT, june 2007.

9 Acknowledgement

The EUWB consortium would like to acknowledge the support of the European Commission partly funding the EUWB project under Grant Agreement FP7-ICT-215669